HTCMC5 Abstract

Creep and Stress-Strain Behavior after Creep for SiC fiber reinforced, Melt-infiltrated SiC Matrix Composites

Gregory N. Morscher, Ohio Aerospace Institute, Cleveland, OH
Vijay Pujar, Goodrich Corporation, Brecksville, OH

Silicon carbide fiber (Hi-Nicalon Type S, Nippon Carbon) reinforced silicon carbide matrix composites containing melt-infiltrated Si were subjected to creep at 1315oC for a number of different stress conditions. This study is aimed at understanding the time-dependent creep behavior of CMCs for desired use-conditions, and also more importantly, how the stress-strain response changes as a result of the time-temperature-stress history of the crept material. For the specimens that did not rupture, fast fracture experiments were performed at 1315oC or at room temperature immediately following tensile creep. In many cases, the stress-strain response and the resulting matrix cracking stress of the composite change due to stress-redistribution between composite constituents during tensile creep. The paper will discuss these results and its implications on applications of these materials for turbine engine components.

CREEP AND STRESS-STRAIN BEHAVIOR AFTER CREEP FOR SIC FIBER REINFORCED, MELT-INFILTRATED SIC MATRIX COMPOSITES

Gregory N. Morscher
Ohio Aerospace Institute
NASA Glenn Research Center
Cleveland, OH

Vijay Pujar
Goodrich Corporation
Brecksville, OH

Work supported by a joint NASA, Goodrich Space Act Agreement

Objective

- To determine the creep behavior of the Hi-Nicalon Type S*, slurry-cast melt-infiltrated (MI) composite system including the retained stress-strain behavior after prolonged tensile creep
  - History dependent σ/ε for modeling purposes
  - Creep-induced matrix compression to raise "proportional limit" stress [1,2]

* Nippon Carbon Co., Japan

Hi-Nicalon Type S, Melt-Infiltrated Composite System

- A very creep resistant and relatively strong fiber
- A relatively high matrix cracking matrix stress composite
  - Slurry SiC + melt Si fills in most of open porosity remaining after CVI SiC
    - Removes (fills in) stress concentrators present in CVI SiC matrix systems
    - Adds compressive stress to matrix due to volume expansion of Si on cooling and thermal expansion difference between Si (~3x10^{-6} /^{o}C) and SiC (~4.5x10^{-6}/^{o}C)

Experimental: Composite Processing

- Composite processing consisted of the following steps:
  - Stacking and BN CVI (interphase) of eight plies of woven fabric
  - SiC CVI in order to rigidize the preform and protect the fibers from melt-infiltration
  - Slurry-infiltration of SiC particles
  - Melt-infiltration of molten Si
- Two different matrix compositions were processed [3]:
  - High CVI SiC & low Si content (A Panels)
  - Low CVI SiC & high Si content (B Panel)

Experimental: Mechanical Behavior

- Tensile tests was performed on 152 mm long dogbone specimens (12.6 mm in grip and 10 mm in gage)
- Unload, reload tensile hysteresis tests were performed at room temperature to determine the residual stress in the matrix
- Elevated temperature tests were loaded monotonically (0.25 mm/min) to failure for fast fracture or to the predetermined load for tensile creep
- If tensile creep survived 100 hours, the specimen was unloaded to zero stress and either reloaded immediately to failure at 1315°C or cooled to room temperature and tensile hysteresis to failure was perfromed
- Elastic modulus was determined from linear regression of the 5 to 50 MPa portion of initial loading of σ/ε curve.
- The 0.002% offset stress was used to characterize non-linearity (proportional limit)

Figure 1: Tensile Creep Curves

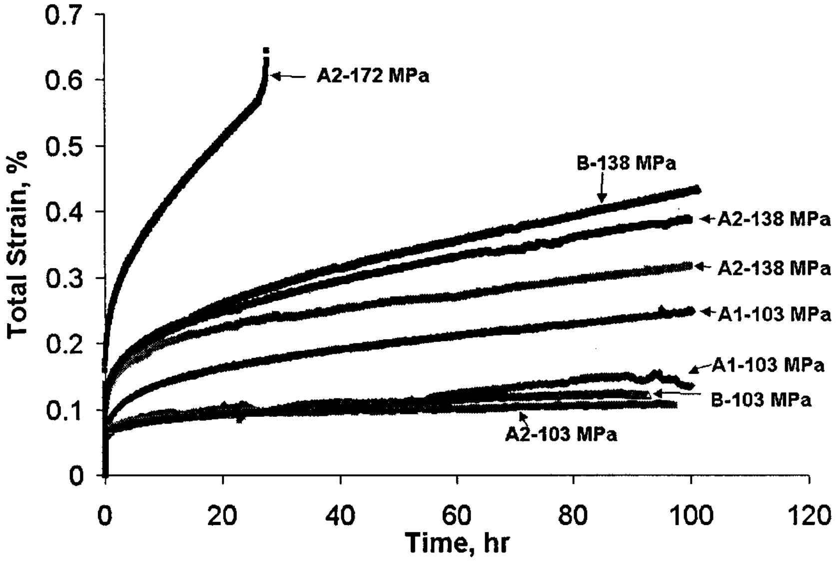

Figure 2: Strain Rate vs. Time

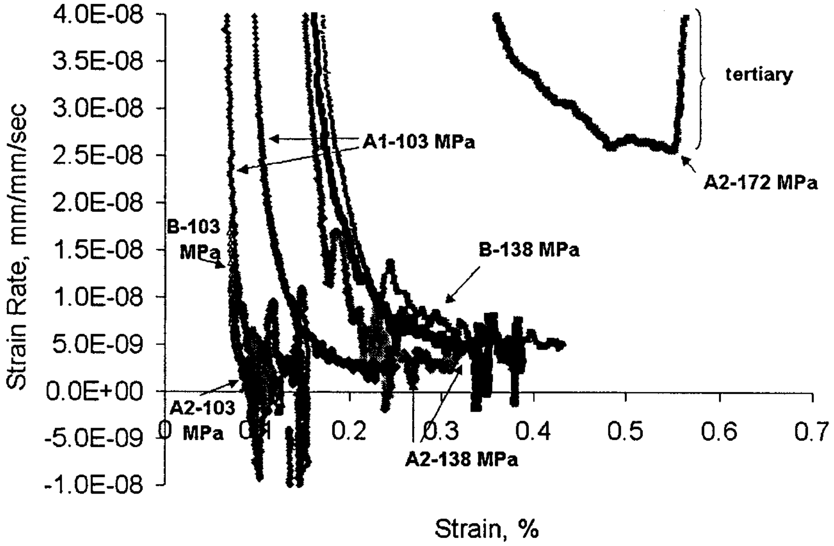

Table I: Tensile Data

Panel	Experi-ment	Creep Stress, MPa	E(RT), GPa	E(1315) Initial Loading, GPa	E(1315) After Creep, GPa	E(RT) after creep	Minimum Strain Rate, sec^{-1}	Creep Strain, %	Ult. Stress, MPa
A1	RT		262						349
	1315FF								253*[X]
	1315Ccreep	103		NA	209		2.80E-09	0.18	256*
	1315Ccreep	103		223	209		2.50E-09	0.09	267*
A2	RT		220						412
	1315FF			182					271*[X]
	1315Ccreep	103		225	198		2.80E-10	0.05	295*
	1315Ccreep	138		184	157		3.90E-09	0.3	291*
	1315Ccreep	138		203		233	3.10E-09	0.23	321[R]
	1315Ccreep	172		177			2.60E-08	0.44[a]	
B	RT		270						362
	1315Ccreep	103		217	208		5.60E-10	0.07	255*
	1315Ccreep	138	263	213			5.20E-09	0.36	

* Tested at 1315°C; [X] Did not fail in hot zone; [a] Prior to the onset of tertiary creep

FF = fast fracture; R = tested at room temperature

Results

- Creep failure within 100 hours only occurred for the 172 MPa condition
- Primary creep dominated the creep-time curves (**Figures 1 and 2**). Perhaps a steady-state was reached for the 138 MPa creep condition.
- Retained strength after 100 hour creep was essentially equal to or greater than the 1315°C fast-fracture strength, even for specimens that exhibited 0.3% time-dependent strain. Although, fast-fracture of as-produced specimens never failed in hot zone for 1315°C testing whereas fast-fracture after creep usually did.

Figure 3: Stress-Strain History for Panel A2

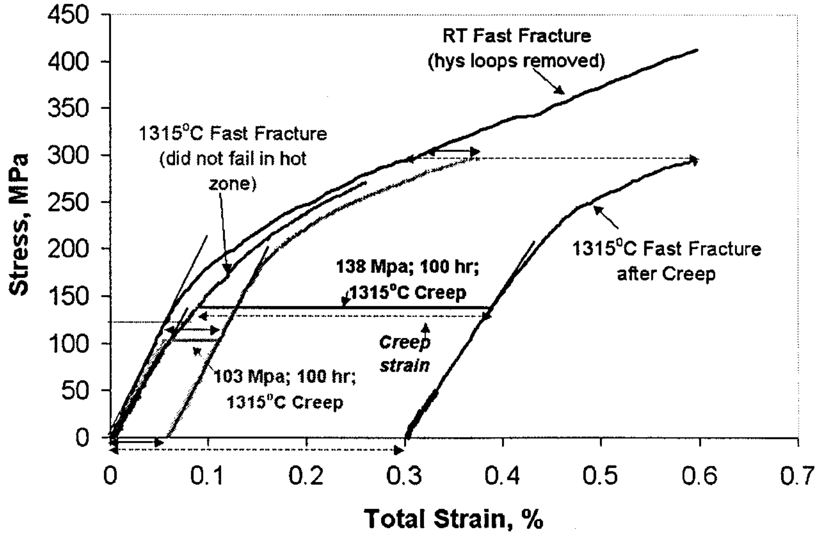

Table II: Offset Stress

			0.002% offset stress	
Panel	Experiment	Creep Stress, MPa	1315C Initial Loading, MPa	1315C After Creep, MPa
A1	1315FF	--	70	
	1315Ccreep	103	NA	127
	1315Ccreep	103	82	147
A2	1315FF	--	103	
	1315Ccreep	103	67	166
	1315Ccreep	138	88	159
	1315Ccreep	138	79	
	1315Ccreep	172	85	
B	1315Ccreep	103	95	112
	1315Ccreep	138	90	

- There is considerable non-linearity in 1315°C loading curve at relatively low stress (> 100 MPa) for the applied loading rate (see **Table II**). This is believed to be due primarily to creep during loading and not matrix cracking due to the absence of significant matrix crack formation (below).
- After tensile creep, reloading specimens resulted in a lower E; however, the "offset stress" was significantly increased **(Table II)**, especially for A panels with the greater CVI SiC content.
- The time-dependent creep strain was essentially identical with the permanent strain measured after unloading from the creep condition and the difference in strain from after-creep fast-fracture and as-produced fast-fracture (see double-sided arrows in **Figure 3**).

Figure 4: Room-temperature tensile after creep (panel A2)

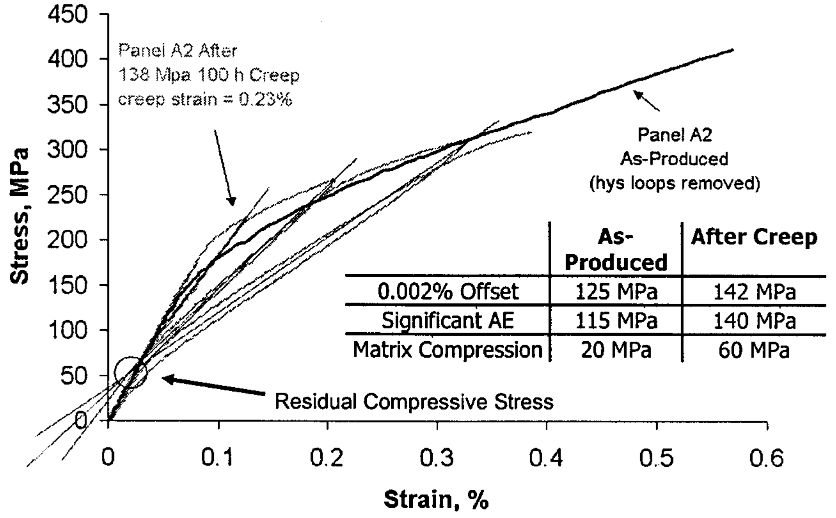

	As-Produced	After Creep
0.002% Offset	125 MPa	142 MPa
Significant AE	115 MPa	140 MPa
Matrix Compression	20 MPa	60 MPa

- Room temperature tensile behavior of after-creep specimen (**Figure 4**) exhibited all the qualities of increased compression in the matrix: higher "proportional limit" stress, higher AE activity stress, and higher residual compressive stress [4].
- Note that very little matrix cracking occurred during creep. For 103 MPa crept specimens, no creep-induced* matrix cracking could be discerned. For 138 MPa crept specimens, a few surface creep-induced microcracks were observed (**Figure 5a**). For the 172 MPa crept specimen, six periodic (spaced ~ 2 mm apart) internal microcracks were observed that resided in the same longitudinal tow three plies from the surface (**Figure 5b**). Several of these caused fiber failure; however, the matrix cracking seemed to not extend beyond the neighboring plies.

* Creep-induced cracking was easy to distinguish from matrix cracking caused during fast fracture. Matrix cracking due to fast-fracture was difficult if not impossible to observe without the aid of plasma etching. Creep-induced matrix cracking exhibited significant opening and oxidation for surface-exposed cracks.

Figure 5: Micrographs of crept specimens.

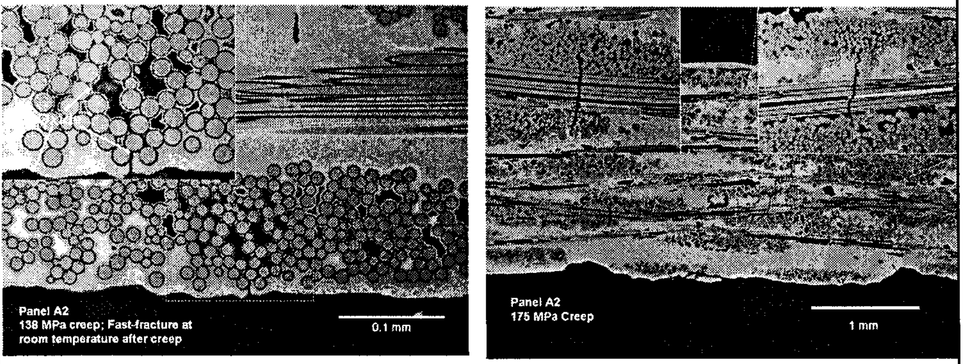

a. Surface microcrack in 138 MPa crept specimen.

b. Internal unbridged microcracks in 172 MPa crept specimen.

Summary and Conclusions

- Woven Hi-Nicalon Type S MI composites exhibit excellent creep resistance at 1315°C and excellent retained properties after 100 hour creep for applied creep stresses up to 138 MPa.
- Tensile creep induced compression in the matrix, presumably due to the relaxation of the MI portion of the matrix which resulted in a higher matrix cracking stress composite.
- It may be possible to take advantage of this creep-induced phenomena for certain high stress applications, e.g., a turbine blade.

References

1. J.W. Holmes, "Influence of Stress Ratio on the Elevated-Temperature Fatigue of a Silicon Carbide Fiber-Reinforced Silicon Nitride Composite," J. Am. Ceram. Soc., 74 [7] 1639-45 (1991)
2. S. Widaja, K. Jakus, J.E. Ritter, E. Lara-Curzio, T.R. Watkins, E.Y. Sun, and J.J. Brennan, "Creep-Induced Residual Strengthening in a Nicalon-Fiber-Reinforced BMAS-Glass-Ceramic-Matrix Composite," J. Am. Ceram. Soc., 82 [3] 657-721 (1999)
3. G.N. Morscher and V.J. Pujar, "Melt-Infiltrated SiC Composites for Gas Turbine Engine Applications," Proceedings of the 49th ASME IGTI Turbo Land, Sea and Air Conference, June 14-17, Vienna Austria, 2004. Paper number: GT2004-53196.
4. M. Steen and J.L. Valles, "Unloading-Reloading Sequences and the Analysis of Mechanical Test Results for Continuous Fiber Ceramic Composites," ASTM STP 1309, M.G. Jenkins et al., Eds. American Society for Testing and Materials, West Conshohocken, PA, 1997, pp. 49-65.